

## Peculiarities in the photophysical properties of some 6-styryl-2,4-disubstituted pyrylium salts

Peter Nikolov<sup>a,\*</sup>, Stefan Metzov<sup>b</sup>

<sup>a</sup> Institute of Organic Chemistry with Centre of Phytochemistry, Bulgarian Academy of Sciences, 1113 Sofia, Bulgaria

<sup>b</sup> Department of Chemistry, Sofia University, 1126 Sofia, Bulgaria

Received 24 November 1999; received in revised form 29 March 2000; accepted 4 April 2000

### Abstract

The absorption and fluorescence characteristics of some 6-styryl-2,4-disubstituted pyrylium salts in cyclohexane, acetonitrile and ethanol are reported. The UV–VIS absorption spectra are dominated by two well separated bands. The absorption band in the spectral region of 320–400 nm for all investigated compounds is strongly localized on the corresponding pyrylium fragment of the molecule, while the longest wavelength absorption band with maximum in the region of 420–530 nm depends on the presence of different substituents in 6-position of the pyrylium fragment. The excitation in the second absorption band (320–400 nm) brings rise to two different emissions, denoted in the text as ‘L’ and ‘D’ bands. The analysis of the experimental data, based on a comparison with the spectral properties of model compounds, show that ‘D’ band is connected with the whole conjugated system of the investigated 6-styryl-2,4-disubstituted pyrylium salts, while ‘L’ band with maximum 400–450 nm is a local emission from the corresponding pyrylium fragment of the molecule. © 2000 Elsevier Science S.A. All rights reserved.

**Keywords:** Electronic spectra; Fluorescence; Local emission; 6-styryl-2,4-disubstituted pyrylium salts

### 1. Introduction

The practical, synthetical and theoretical interest in pyrylium salts (PS) has different reasons. Together with being starting compounds for many syntheses [1,2], their fluorescence characteristics make them applicable as laser dyes, Q-switchers [3–5], organic luminophores with high photostability [6]. Some styryl PS are used as NIR-absorbing dyes [7–9], pH-sensors [9] and PAN-textile dyes [10].

The peculiarities in the photophysical properties of differently substituted pyrylium salts have been discussed in many studies [11–30]. In [11–20], 2,4,6-trisubstituted PS with three identical substituents, e.g. 2,4,6-triaryl PS, as well as some blocked PS are considered as two-dimensional chromophore systems with X- and Y-absorption bands. The optical properties of triarylpyrylium dimmers are discussed in [18–20]. Czerney et al. have studied VIS/NIR absorption/emission behavior of 3,1'-bridged-2,4,6- trisubstituted pyrylium dyes [21]. PS bearing biphenyl groups have remarkable Stock's shift and multiple fluorescence [22]. The

appearance of dual fluorescence is reported in [16,23–27]. The authors in [28] discuss a theoretical model for photoinduced intramolecular CT processes, which should lead to dual fluorescence. The TICT-hypotheses [29] is applied for interpretation of the peculiarities in the fluorescence properties of some triarylpyrylium cations [14,15,23,25]. Kossanyi et al. [24–26] report the dual fluorescence from blocked pyrylium salts (N\* and A\* emissions), which corresponds to two excited states differing from each other by their configuration.

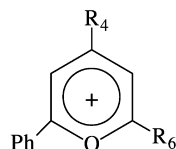
In the present paper, we report for dual emission, observed from the solutions of 6-styryl-, 6-(*p*-substituted) styryl- and 6-(butadiene-yl-phenyl)-2,4-disubstituted PS in solvents of different polarity.

### 2. Experimental details

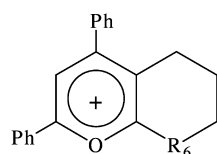
Scheme 1 shows the structure of the investigated compounds. In the course of the discussion of the experimental results, we shall indicate compounds **1**, **2**, **3** and **4** which have a methyl (or methylene) group in position 6, as model compounds for the rest of the PS, with ‘extended X-chromophore’ [13], that have differently *p*-substituted

\* Corresponding author. Fax: +359-2-700225.

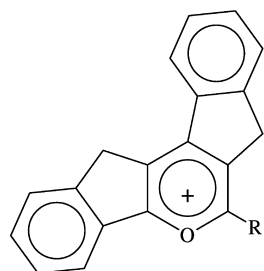
E-mail address: petnik@orgchm.bas.bg (P. Nikolov)



Compound	R <sub>4</sub>	R <sub>6</sub>
<b>1</b>	CH <sub>3</sub>	CH <sub>3</sub>
<b>1a</b>	CH <sub>3</sub>	CH=CH-C <sub>6</sub> H <sub>4</sub> -OCH <sub>3</sub> -p
<b>2</b>	Ph	CH <sub>3</sub>
<b>2a</b>	Ph	CH=CH-C <sub>6</sub> H <sub>4</sub> -OCH <sub>3</sub> -p
<b>2b</b>	Ph	CH=CH-C <sub>6</sub> H <sub>4</sub> -CH <sub>3</sub> -p
<b>2c</b>	Ph	CH=CH-C <sub>6</sub> H <sub>5</sub>
<b>2d</b>	Ph	CH=CH-C <sub>6</sub> H <sub>4</sub> -F
<b>2e</b>	Ph	CH=CH-C <sub>6</sub> H <sub>4</sub> -CN
<b>2f</b>	Ph	CH=CH-CH=CH-C <sub>6</sub> H <sub>5</sub>



Compound	R <sub>6</sub>
<b>3</b>	CH <sub>2</sub>
<b>3a</b>	C=CH-C <sub>6</sub> H <sub>5</sub>



Compound	R <sub>6</sub>
<b>4</b>	CH <sub>3</sub>
<b>4a</b>	CH=CH-C <sub>6</sub> H <sub>4</sub> -OCH <sub>3</sub>

Scheme 1. Structure and R-substituents of the investigated compounds.

styryl fragment  $-\text{CH}=\text{CH}-\text{C}_6\text{H}_4-\text{R}$  (R=H, OCH<sub>3</sub>, CH<sub>3</sub>, F, CN) or  $-\text{CH}=\text{CH}-\text{CH}=\text{CH}-\text{Ph}$  fragment in position 6.

The model compounds **1**, **2**, **3** and **4** are synthesized according to standard procedures [2,10].

The 6-styryl-substituted PS are synthesized by condensation of the corresponding model compound with aldehydes by boiling under reflux in glacial acetic acid (in some cases with a few acetic anhydride) from 4 to 6 h, the yields are above 85% (general procedure).

### 2.1. Compound **2a**

In two-neck round-bottom flask fitted with reflux and stirrer, 3.5 g (0.01 mol) 6-methyl-2,4-diphenylpyrylium perchlorate are fully dissolved in 200 ml boiling acetic acid. Into this solution are added 12.5 ml (0.01 mol) anisaldehyde and reaction mixture boils under reflux by stirring at about 5 h. After cooling the obtained 6-(*p*-methoxystyryl)-2,4-diphenylpyrylium perchlorate is filtered, washed with a little acetic acid, ethanol, ether and dried. Yield: 88% crude product, mp 232–5°C; after recrystallization (twice) from acetic acid mp 235–6°C. TLC data:

$R_f=0.66$ ; liquid phase CHCl<sub>3</sub>: CH<sub>3</sub>COCH<sub>3</sub>: CH<sub>3</sub>COOH: HCOOH: (CHH<sub>5</sub>)<sub>2</sub>O=8:6:1:1:16 on plate of Kieselgel 60F250.

Elemental analysis (examples): compound **2a** — calculated: %C=67.17;%H=4.52. Found: %C=63.73; %H=4.57. After recalculating the molecular formula with 2 molecules H<sub>2</sub>O, the results are: calculated: %C=63.48; %H=4.88. Compound **2f** — calculated: %C=70.36; %H=4.56. Found: %C=65.88; %H=5.49. After recalculating the molecular formula with 2 molecules H<sub>2</sub>O, the results are: calculated: %C=65.25; %H=5.35.

All compounds are recrystallized until a constant melting point is obtained and are characterized by elemental analysis, NMR, IR, absorption and fluorescence spectra. The presented data for the electronic spectra of the investigated compounds refer to freshly prepared solutions.

### 2.2. IR spectral data

The IR spectra of the investigated compounds are recorded on Bruker IFS 113 v Spectrometer in KBr tablets. According to the literature data [31,32], the skeleton vibra-

tions of the pyrylium ring are in the range 1650–1630  $\text{cm}^{-1}$ . In the studied compounds, we found the following frequencies: compound **1** — 1637  $\text{cm}^{-1}$ ; compound **2** — 1630  $\text{cm}^{-1}$ ; compound **1a** — 1633  $\text{cm}^{-1}$  compound **2a** — 1630  $\text{cm}^{-1}$  compound **2e** — 1631  $\text{cm}^{-1}$  compound **2f** — 1630  $\text{cm}^{-1}$ . The intensive band corresponding to the C–O–C bound in the pyrylium ring is observed at: compound **1** — 1083  $\text{cm}^{-1}$ ; compound **2** — 1085  $\text{cm}^{-1}$ ; compound **1a** — 1092  $\text{cm}^{-1}$ ; compound **2a** — 1086  $\text{cm}^{-1}$ ; compound **2e** — 1087  $\text{cm}^{-1}$ ; compound **2f** — 1087  $\text{cm}^{-1}$ . The vibrations of the other ether bound Ar–O–Me in compounds **1a** and **2a** are 1165, 1258 and 1514  $\text{cm}^{-1}$  (compound **1a**) and 1171, 1271 and 1516  $\text{cm}^{-1}$  (compound **2a**). In the IR spectra of compounds **1**, **2** and **1a**, a band in the range 1470–1480  $\text{cm}^{-1}$  is observed, due to the asymmetric deformational modes of the methyl group(s), present in the pyrylium fragment: 1480  $\text{cm}^{-1}$  (compound **1**), 1478  $\text{cm}^{-1}$  (compound **2**), 1473  $\text{cm}^{-1}$  (compound **1a**). We observed a band at 2226  $\text{cm}^{-1}$  in the spectrum of compound **1e** due to the presence of CN-group. The band, corresponding to the double bound stretching vibrations in the spectra of compounds **1a** and **2a–2f** is strongly overlapped by the benzene rings bands present.

### 2.3. NMR spectral data

The  $^1\text{H}$ -NMR spectra are recorded on a Tesla BS 487C (80 MHz) spectrometer with trifluoroacetic acid (TFA) as a solvent. Chemical shifts are measured in parts per million (ppm) with respect to internal standard TMS, in some cases DMSO- $d_6$ /HMDSO are used. The results for some compounds instigated are as follows:

Compound **1** (TFA), ppm: 2.99 (s, 3H,  $\text{CH}_3$ -4); 3.20 (s, 3H,  $\text{CH}_3$ -6); 7.65–8.60 (m, 5H, Ar); 8.75 (s, 2H, Pyr H-3,5);

Compound **2** (DMSO- $d_6$ ), ppm: 3.25 (s, 3H,  $\text{CH}_3$ ); 7.25–8.74 (m, 10H, Ar); 8.81 (s, 1H, Pyr H-5); 9.27 (s, 1H, Pyr H-3);

Compound **4** (TFA), ppm: 3.20 (s, 3H,  $\text{CH}_3$ ); 4.38 (s, 2H,  $\text{CH}_2$ -5); 4.55 (s, 2H,  $\text{CH}_2$ -3); 7.50–8.45 (in, 8H, Ar).

The signal for the 6-methyl group in compounds **1**, **2** and **4** is observed in the range 3.2–3.25 ppm; this value is very closed to the chemical shifts of  $\text{CH}_3$ -groups in compounds with similar structure [33]. The positions of the pyrylium protons, about 9 ppm, are also in accordance to the literature data [34]. In the spectrum of compound **4** where all positions of the pyrylium ring are substituted, no signals for pyrylium protons (Pyr H) are observed.

Compound **2a** (DMSO- $d_6$ ), ppm: 3.83 (s, 3H,  $\text{OCH}_3$ ); 7.22–8.70 (m, 16H, Ar, CH CH); 8.79 (s, 1H, Pyr H-5); 9.23 (s, 1H, Pyr H-3);

Compound **4a** (TFA), ppm: 3.78 (s, 3H,  $\text{OCH}_3$ ); 4.37 (s, 2H,  $\text{CH}_2$ -5); 4.50 (s, 2H,  $\text{CH}_2$ -3); 7.60–8.50 (in, 14H, Ar, CH=CH).

Contrary to the spectra of the starting compounds **1**, **2** and **4**, no signals for 6- $\text{CH}_3$ -groups in compounds **2a** and **4a** are recorded.

The absorption spectra are recorded on a SPECORD M40 (Carl Zeiss, Jena). The corrected excitation and fluorescence spectra are taken on a Perkin-Elmer MPF 44 spectrofluorimeter. The fluorescence quantum yields ( $Q_f$ ) are measured relatively to 3-amino-phthalimide ( $Q_f=0.6$  in ethanol) [35]. The solvents used are of fluorescence grade. The fluorescence decay curves are measured in solution at room temperature 25°C with a nanosecond Single Photon Counting spectrofluorimeter System PRA 2000, using a nitrogen filling flash lamp with FWHM about 2.5 ns, excitation wavelength=356 nm, the emission wavelength corresponds to the maximum of the fluorescence band (see the text), time-resolution=0.1 ns per channel, all collected decay curves have 10,000 counts in the maximum. The fluorescence lifetimes  $\tau_f$  are calculated from the decay curves using the method of non-linear least-squares curve fitting. The goodness of the fit is controlled by the weighted residuals, the autocorrelation function of the residuals and the reduced chi-square.

## 3. Results and discussion

### 3.1. Absorption

#### 3.1.1. Absorption of the model compounds

The longest wavelength absorption band of the model compounds **1**, **2**, **3** and **4** is in the region 300–400 nm, depends on the substituent ( $-\text{Ph}$  or  $-\text{CH}_3$ ) in position 4 in the pyrylium ring, the presence of methylene bridges (compounds **3** and **4**) and the solvent polarity — dichloromethane (DCM), acetonitrile (AN) and ethanol (ETOH) (Table 1).

In the model compound **4**, where the two phenyl substituents in positions 2- and 4- in the pyrylium ring are fixed by methylene bridges, the absorption band is bathochromically shifted in comparison with compound **2**, where the two Ph substituents are free for rotation. For instance, in DCM the absorption maxima of **2** and **4** are at 383 nm and 400 nm, respectively. The observed lowering of the absorption energy in compound **4** should be attributed to increasing of the conjugation in the fixed structure that enhances the CT from the pyrylium O-atom to the both 2,4-phenyl groups [16].

#### 3.1.2. Absorption of the 6-styryl-2,4-disubstituted pyrylium salts

The absorption spectrum of all investigated 6-styryl-substituted PS is characterized by two bands in the spectral region 300–600 nm (Table 1, Figs. 1–4).

The longest wavelength absorption band of the 6-styryl-substituted PS has maximum in the spectral region 450–550 nm, the band is bathochromically shifted at least by 5000  $\text{cm}^{-1}$  in comparison to the corresponding model compound. The energy of the longest wavelength absorption maximum, as well as its relative intensity strongly depends on the substituent R in the styryl fragment, but also on the substituents in 2- and 4-position in the pyrylium ring

Table 1

Absorption maxima (in nm) of the investigated compounds in DCM, AN and ETOH in the region 300–600 nm<sup>a</sup>

Compound	DCM	AN	ETOH
<b>1</b>	360	345	336
<b>1a</b>	360+505 (max)	345 (-)+466 (max)	320+480 (max)
<b>2</b>	346+383 (max)	332+368 (max)	330 (max)+373
<b>2a</b>	383 (max)+529	368 (max)+498	330 (max)+373+507
<b>2b</b>	383 (max)+487	368 (max)+450	330 (max)+370 (s)+450
<b>2c</b>	383 (max)+470	368 (max)+423	330+373 (max)+450
<b>2d</b>	383 (max)+472	368 (max)+451	373 (max)+430
<b>2e</b>	383 (max)+460	368 (max)+445	330+373 (max)+450
<b>2f</b>	383 (max)+526	368 (max)+496	330 (max)+373 (s)+504
<b>3</b>	377	370	335 (max)+368
<b>3a</b>	377 (max)+470	366 (max)+460	335 (max)+430
<b>4</b>	400	335 (max)+389	336+392 (max)
<b>4a</b>	400 (max)+530	335 (max)+505	336 (max)+390 (s)+505

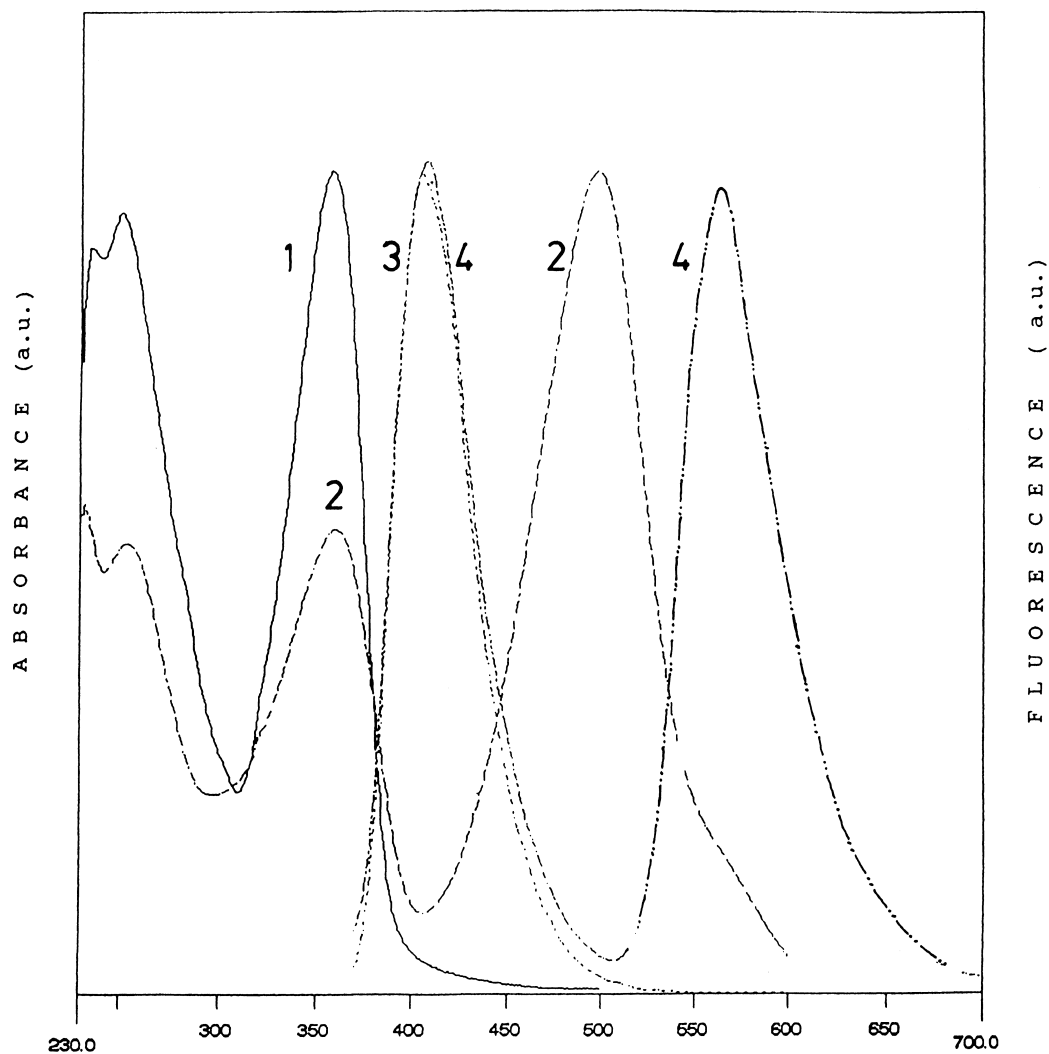
<sup>a</sup> (max) denotes the most intensive band.

Fig. 1. Absorption and fluorescence spectra ( $\lambda_{\text{ex}}=360$  nm) of compounds **1** and **1a** in DCM (normalized to 1). Curve 1 (—): compound **1**, absorption; curve 2 (---): compound **1a**, absorption; curve 3 (-·-·-): compound **1**, fluorescence; curve 4 (·····): compound **1a**, fluorescence.

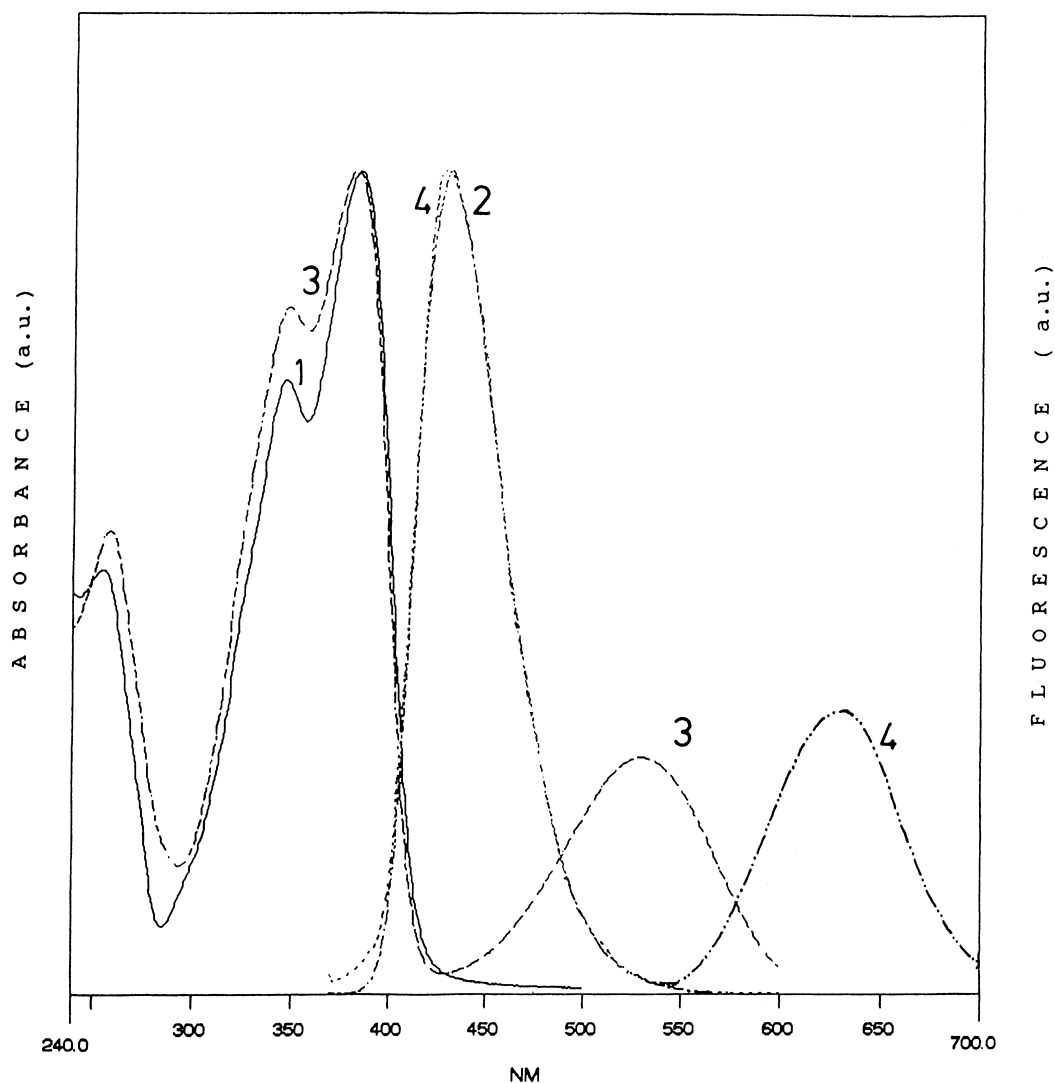


Fig. 2. Absorption and fluorescence spectra ( $\lambda_{\text{ex}}=360$  nm) of compounds **2** and **2a** in DCM (normalized to 1). Curve 1 (—): compound **2**, absorption; curve 2 (---): compound **2**, fluorescence curve 3 (···): compound **2a**, absorption curve 4 (-·-·-): compound **2a**, fluorescence.

(refer for instance, the data for **1a**, **2a**, **2c** in Table 1 and Figs. 1–3). The results indicate that the longest wavelength absorption band of the 6-styryl-2,4-disubstituted PS is determined by the whole conjugated system, including both the pyrylium ring and the corresponding styryl fragment.

The positive charge, localized on the pyrylium ring determines the bathochromic shift of the longest wavelength absorption maxima for the electron-donating substituents  $R = -\text{OCH}_3$ ,  $-\text{CH}_3$  (compounds **2a** and **2b**) in comparison to  $R = -\text{H}$ ,  $-\text{CN}$  and  $-\text{F}$  (compounds **2c**, **2e** and **2d**), indicating the CT character of this band (Table 1). The prolongation of the 6-styryl fragment with one more vinylene group — compound **2f** — leads to decreasing the energy of the longest wavelength absorption maxima similar to the effect of the  $p\text{-OCH}_3$  group in compound **2a** (Fig. 3, Table 1).

The second absorption band of the investigated 6-styryl and 6-(butadiene-yl-phenyl)-2,4-disubstituted PS is in the

spectral region 300–400 nm. The energy, shape and vibronic structure of this band correspond to the characteristics of the longest wavelength absorption band of the model compound (Figs. 1–3, Table 1). The effect of the substituents in 6-position of the pyrylium ring on the characteristics of the second absorption band in DCM is limited only to a small changes in the relative intensity of the vibronic bands (refer for the spectra in Figs. 1–3). In polar solvents (AN, ETOH), this effect is more pronounced and in some cases — **2b**, **3**, **3a**, **4**, **4a** — leads to change in the relative intensity of the two vibronic bands. As a final result, the absorption maximum in polar solvents is shifted hypsochromically in comparison to the maximum in DCM (Table 1). Fig. 4 illustrates the effect of the solvent polarity on the absorption spectra of compound **2b**.

The second absorption band of compound **1a** in AN and ETOH, which corresponds to the absorption of the model

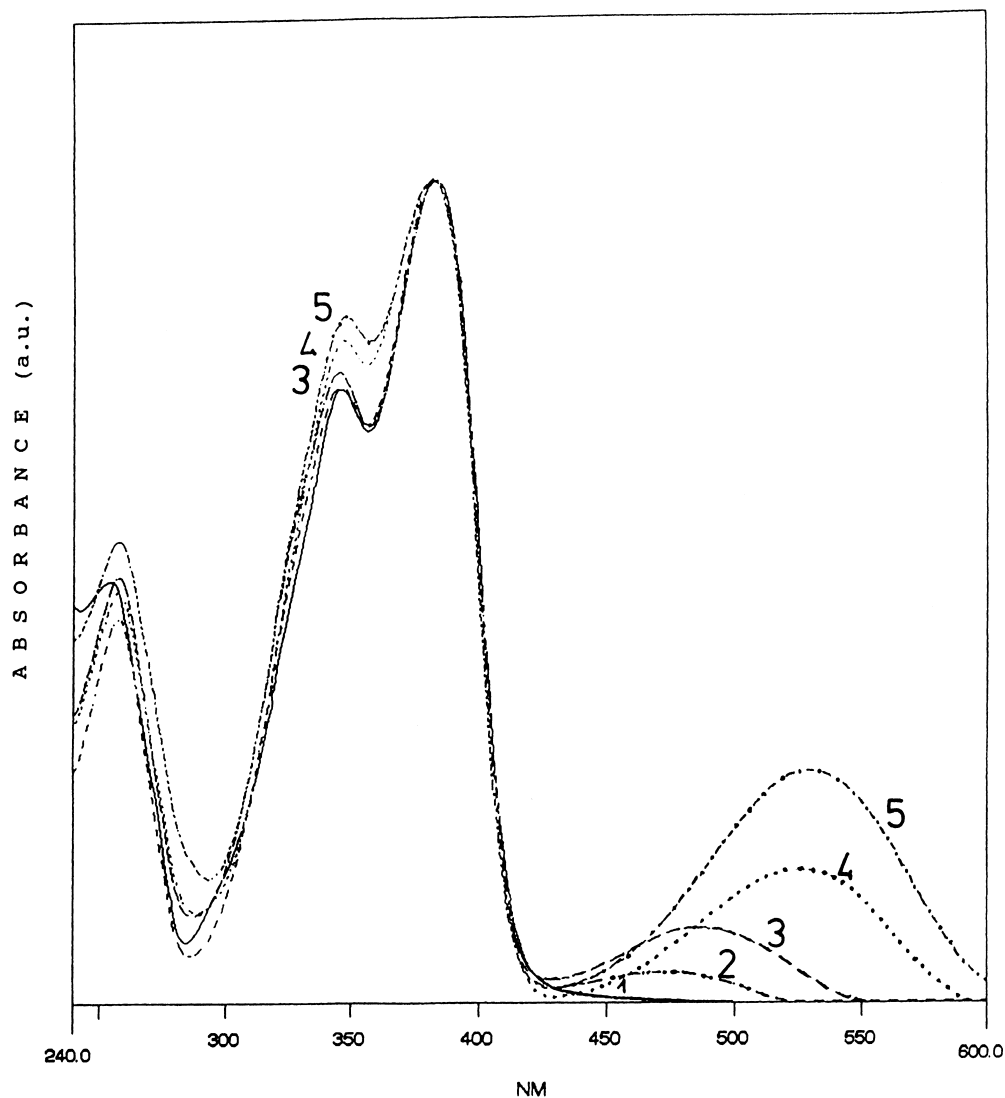


Fig. 3. Absorption spectra of compounds **2**, **2a**, **2b**, **2d** and **2f** in DCM (normalized to 1). Curve 1 (—): compound **2**, absorption; curve 2 (— · — · —): compound **2d**, absorption; curve 3 (---): compound **2b**, absorption; curve 4 (····): compound **2f**, absorption; curve 5 (— — —): compound **2a**, absorption.

compound **1** is not clearly presented in the spectra of **1a**, these cases are denoted in Table 1 with (—).

The analysis of the experimental results leads to the conclusion that the second absorption transition in the 6-styryl and 6-butadienophenyl PS is localized on the pyrylium fragment of the molecule. Similar strong localization of the second absorption band on one molecular fragment was reported also for some benzylidenephthalides [36].

In line with the literature data for other substituted PS [13,30], both the absorption bands shift weakly hypsochromically with increasing the solvent polarity (DCM, AN, ETOH) (see Table 1).

### 3.2. Steady-state fluorescence

The fluorescence characteristics of the investigated compounds in dichloromethane, acetonitrile and ethanol are

compiled in Table 2. The fluorescence spectra for some typical cases are presented in Figs. 1, 2, 5 and 6.

#### 3.2.1. Fluorescence of the model compounds

For the model compounds **1**, **2**, **3** and **4**, the excitation with 360 nm, which is in the region of their longest wavelength absorption band, gives rise to fluorescence with maximum in the region 400–440 nm (Table 2, Figs. 1, 2 and 5). The excitation spectrum corresponds to the absorption one (Fig. 7). On contrary to the absorption, increasing the solvent polarity shifts the fluorescence maxima to the red with no more than 10 nm (Table 2).

With the exception of compound **3**, the fluorescence quantum yields increase with the solvent polarity (DCM–AN) (Table 2). Changing the proton-donating ability of the polar solvent, i.e. replacing acetonitrile by hydrogen bonding solvents like ethanol, results in a remarkable decreasing of

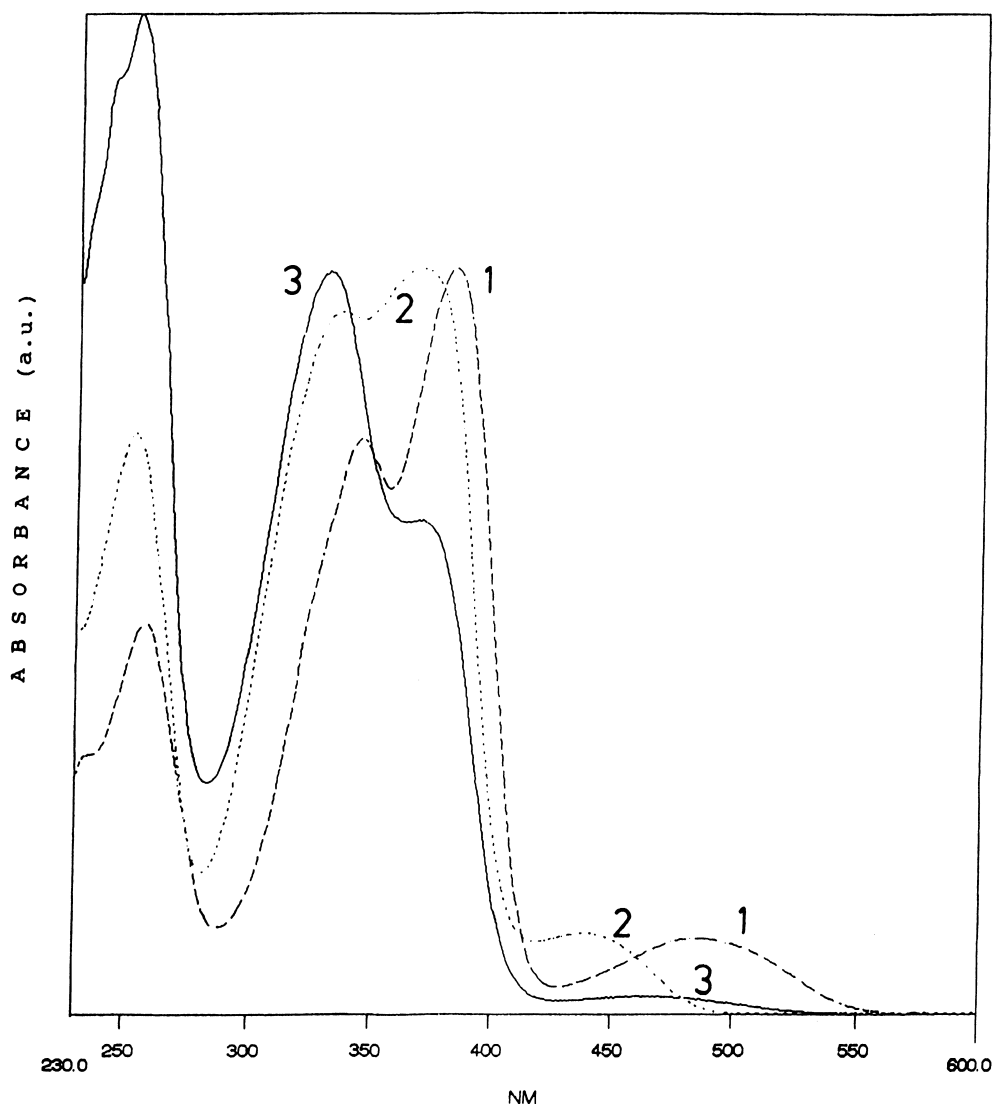


Fig. 4. Absorption spectra of compound **2b** in DCM, AN and ETOH (normalized to 1). Curve 1 (—): compound **2b** absorption in DCM; curve 2 (···): compound **2b**, absorption in AN; curve 3 (---): compound **2b**, absorption in ETOH.

the fluorescent intensity;  $Q_f$  in ETOH diminishes at least by one order of magnitude in comparison to DCM and AN (Table 2). This effect indicates for a specific solute–solvent interaction in the excited state in protic solvents, most probably to forming of non-fluorescent excited complexes [37].

### 3.2.2. Fluorescence of the 6-styryl-2,4-disubstituted pyrylium salts

Upon excitation the solutions of the investigated 6-styryl-2,4-disubstituted PS in their longest wavelength absorption band ( $\lambda_{ex} > 450$  nm) a fluorescence band with maximum in the spectral region 470–650 nm is observed. The Stock's shift of this emission is less than  $3000\text{ cm}^{-1}$ , the shape of the emission band shows a mirror symmetry to the absorption. The excitation spectrum corresponds to the absorption in the whole spectral region after 250 nm. Similar to the longest wavelength absorption band, the

energy of the fluorescence maximum strongly depends on the substituent R in the styryl fragment (Table 2). In Fig. 6 are presented the fluorescence bands of compounds **2a**, **2b**, **2c**, **2d**, **2e** and **2f** in DCM, after excitation in the region of their longest wavelength absorption band.

The excitation in the second absorption band of the 6-styryl-substituted PS (330–400 nm) that coincides to the longest wavelength absorption transition of the corresponding model compound, leads to appearance of two different emission bands. In Table 2, the fluorescence maxima  $\lambda_f$  and the corresponding fluorescence quantum yields  $Q_f$  in DCM, AN and ETOH of the both bands after excitation with 360 nm are presented. It must be mentioned that the energy of the maximum and the shape of the both emission bands do not depend on the excitation wavelength in the whole region of the second absorption band of the 6-styryl-substituted PS.

Table 2

Fluorescence maxima  $\lambda_f$  (in nm) and fluorescence quantum yields,  $Q_f$ , of the investigated compounds in DCM, AN and ETOH at room temperature<sup>a</sup>

Compound	DCM		AN		ETOH	
	Band 'L' ( $\lambda_f/Q_f$ )	Band 'D' ( $\lambda_f/Q_f$ )	Band 'L' ( $\lambda_f/Q_f$ )	Band 'D' ( $\lambda_f/Q_f$ )	Band 'L' ( $\lambda_f/Q_f$ )	Band 'D' ( $\lambda_f/Q_f$ )
<b>1</b>	404/0.38	/ <sup>b</sup>	410/0.56	/	412 / 0.03	/
<b>1a</b>	404/0.06	565/0.06	410/0.04	570/**c	412/0.001	570/0.002
<b>2</b>	430/0.34	/	437/0.72	/	440/0.02	/
<b>2a</b>	430/0.18	630/0.06	440/0.48	640/**	440/**	645/**
<b>2b</b>	429/0.23	570/0.05	440/0.53	582/**	440/0.01	570/0.012
<b>2c</b>	430/0.28	540/**	437/0.70	575/**	440/0.02	555/0.004
<b>2d</b>	430/0.2	550/**	440/0.43	555/**	440/0.008	556/0.016
<b>2e</b>	430/0.10	520/**	440/0.50	513/**	440/**	520/0.001
<b>2f</b>	430/0.21	620/0.05	440/0.40	630/0.02	440/0.009	625/0.031
<b>3</b>	425/0.44	/	435/0.34	/	440/**	/
<b>3a</b>	425/0.40	560/**	435/0.33	560/**	410/**	560/**
<b>4</b>	425/0.47	/	425/0.60	/	425/0.006	/
<b>4a</b>	425/0.47	630/**	425/0.60	630/**	425/0.006	580/**

<sup>a</sup> The excitation wavelength for all the cases is 360 nm. The first column for every solvent refers to the band 'L' and the second one to the band 'D' (see the text).

<sup>b</sup> Indicates the absence of 'D'-band in this compound.

<sup>c</sup> Indicates  $Q_f$  values less than 0.001.

The first emission band that arises after excitation with 360 nm has maximum in the spectral region 400–440 nm, its position and shape are very closed to the fluorescence of the corresponding model compound (Figs. 1, 2 and 5) and the excitation spectrum repeats the absorption one. Later in the text this emission will be marked as 'L'-band.

The second emission band observed after excitation with 360 nm is identical to the fluorescence that appears after excitation of the investigated 6-styryl-substituted PS in the region of their longest wavelength absorption band (i.e. with  $\lambda_{ex} \geq 450$  nm) (Figs. 1, 2, 5 and 6). This emission will be marked in the text as 'D'-band.

**3.2.2.1. 'D'-band.** The energy of the fluorescence maximum and the fluorescence quantum yield of 'D'-band depend on the changes in the two main fragments of the molecule: the 6-styryl moiety and the 2,4-disubstituted pyrylium ring. The effects could be followed for instance by comparison of the fluorescence characteristics of compounds **2c**, **2b**, **2a**, **2e** and **2d** and compounds **1a** and **4a**.

The fluorescence maximum of 'D'-band in the 6-styryl-substituted pyrylium salts **2a–2e** shifts bathochromically with introducing electron-donating substituents R and is only weakly influenced by electron-acceptors (Table 2, Fig. 6). For instance, the fluorescence maxima of **2c** (R=H), **2b** (R=CH<sub>3</sub>) and **2a** (R=OCH<sub>3</sub>) in DCM are 543, 570 and 630 nm, the corresponding values of  $Q_f$  are less than  $10^{-3}$ , 0.05 and 0.06, similar effects are observed also in AN and ETOH. Fig. 5 illustrates the effect of the substituents in the 6-position of the pyrylium ring on the fluorescence spectra after excitation with  $\lambda_{ex}=360$  nm of compounds **2**, **2a**, **2b**, **2c**, **2e** and **2f** in ETOH. For compounds **1a** and **4a** that have identical styryl substituent R (–CH=CH–C<sub>6</sub>H<sub>4</sub>–OCH<sub>3</sub>–p) in position 6, but different structure of the pyrylium fragment, the corresponding data in DCM are:  $\lambda_f=565$  and 630 nm,

$Q_f=0.06$  and less than  $10^{-3}$ , respectively. All these experimental results prove that similarly to the longest wavelength absorption band, the fluorescence band 'D' is unambiguously connected to the whole conjugated system of the investigated 6-styryl-substituted pyrylium salts.

**3.2.2.2. L-band.** On the contrary to the emission 'D', the origin of the observed fluorescence band 'L' is not trivial. Bearing in mind the absorption spectrum of the 6-styryl-substituted PS, the fluorescence band 'L' is quite unusually positioned, as illustrated in Figs. 1 and 2, this emission appears to be with higher energy than the longest wavelength absorption band of the corresponding 6-styryl-substituted compound.

For most of the compounds investigated (the only exception is **1a**), the fluorescence band 'L' dominates the emission spectrum in DCM and AN after excitation with 360 nm, being much more intensive than the fluorescence 'D' that is 'normally' positioned (bathochromically shifted against the longest wavelength absorption band of the 6-styryl-substituted PS). In ETOH, the fluorescence band 'D' dominates the emission spectrum of compounds **1a**, **2a**, **2b**, **2d**, **2e** and **2f** (see the data in Table 2 and Fig. 5). In some cases, the overlapping of the two emission bands with strongly different intensity makes impossible the correct identification of  $\lambda_f$  and  $Q_f$  for the 'D' band. In Table 2 these cases are indicated by (\*\*\*) and their  $\lambda_f$  values are determined after excitation in the region of the longest wavelength absorption band.

The fluorescence band 'L' arises after excitation in the second absorption band (300–400 nm) of the investigated 6-styryl-substituted pyrylium salts that is strongly localized only on the pyrylium fragment of the molecule (see Section 3.1.2). The fluorescence maximum and the shape of the fluorescence band 'L' are practically identical to the fluores-



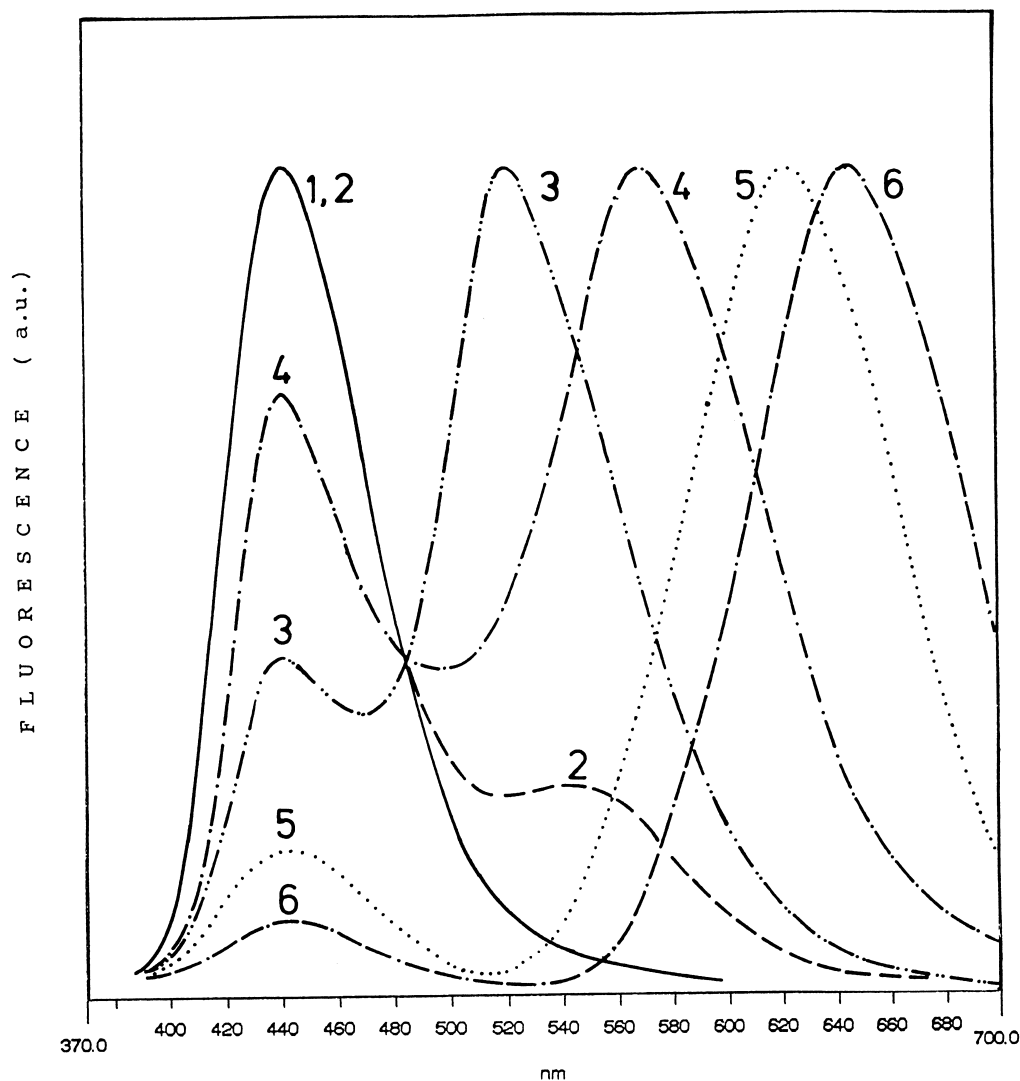


Fig. 5. Fluorescence spectra ( $\lambda_{\text{ex}}=360$  nm) of compounds **2**, **2a**, **2b**, **2c**, **2e** and **2f** in ETOH (normalized to 1). Curve 1 (—): compound **2**; curve 2 (---): compound **2c**; curve 3 (-·-·-): compound **2e**; curve 4 (- - -): compound **2b**; curve 5 (····): compound **2f**; curve 6 (- - -): compound **2a**.

cence of the corresponding model compound and does not depend on the nature of the *p*-substituted 6-styryl fragments in the pyrylium ring (Figs. 1, 2 and 5). On the other hand, the presence of this substituent remarkably influences the fluorescence quantum yield of 'L' which is lower or equal, but never higher than the  $Q_f$  of the model compound (Table 2). For instance, in the cases of **2a**, **2c** and **2e** the fluorescence quantum yield of 'L' in DCM is 0.18, 0.28, 0.1, while  $Q_f$  of **2** in DCM is 0.34.

### 3.2.3. Polarization spectra

The polarisation degree  $P_0$ , calculated from the polarization excitation spectra, clearly distinguishes the two electronic transitions in the absorption spectrum of the investigated pyrylium salts. Fig. 7 presents the  $P_0$  values in the case frozen ethanol solution at 77 K of compound **1a**.

If the emission is fixed at 540 nm, which corresponds to the fluorescence band 'D', the polarization degree is

$P_0=+0.3$  in the spectral region of the longest wavelength absorption band (440–500 nm), and  $P_0=-0.2$  in the spectral region of the second absorption band (320–360 nm). Using the Perrin's equation [38]

$$P_0 = \frac{3 \cos^2 \beta - 1}{\cos^2 \beta + 3}$$

the calculated angles  $\beta$  between the oscillator of the emission band 'D' and the oscillators of the two absorption bands are  $\beta_1=\pm 32^\circ + \pi$  and  $\beta_2=\pm 69^\circ + \pi$ , respectively.

If the emission is fixed at 450 nm, which corresponds to the fluorescence band 'L', the polarization degree in the spectral region of the second absorption band (320–360 nm) is  $P_0=-0.1$  and the corresponding magnitude of  $\beta$  is  $\beta_3=\pm 62^\circ + \pi$ . The indefinite sign of  $\beta$  does not allow the fixing of the difference between the transition moments of the two absorption bands.

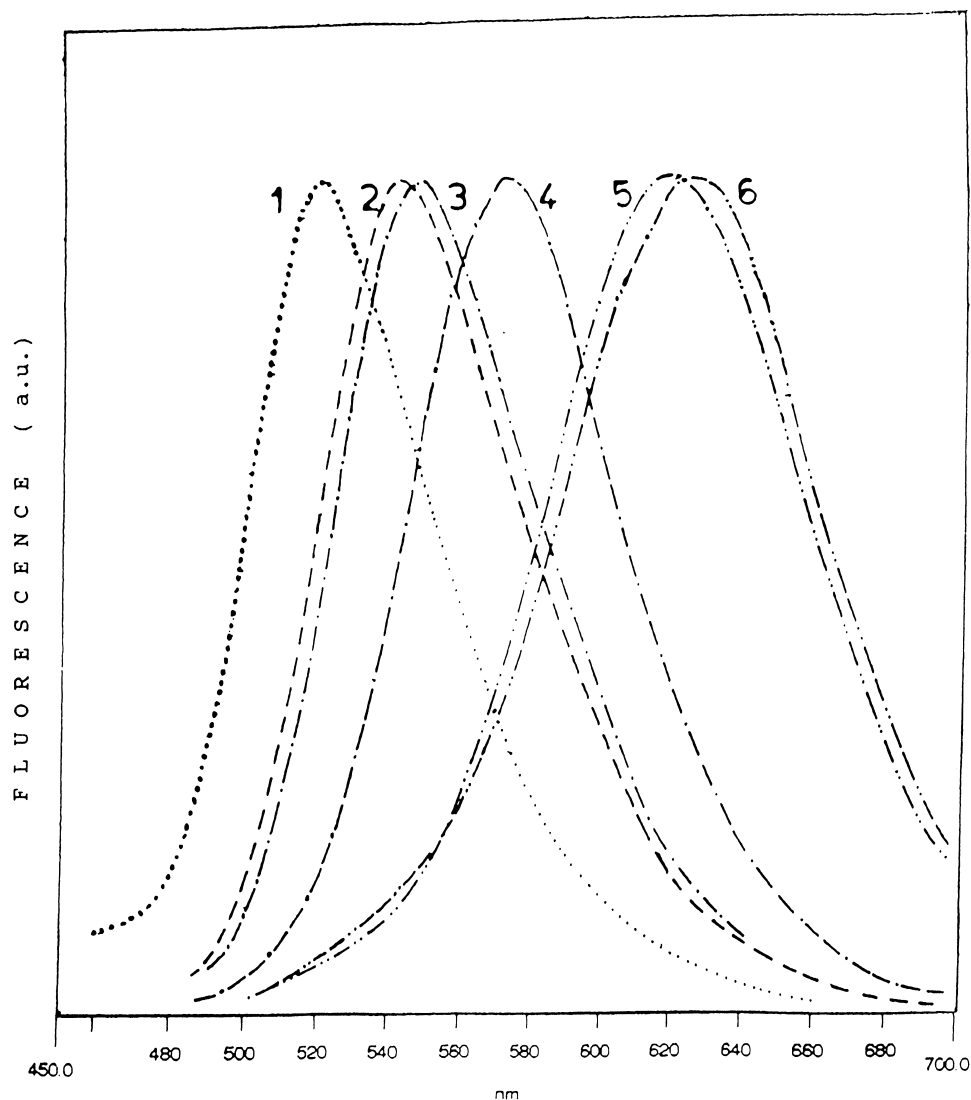


Fig. 6. Fluorescence spectra (band 'D') of compounds **2a**, **2b**, **2c**, **2d**, **2e** and **2f** in DCM (normalized to 1). The excitation wavelength for every spectrum corresponds to the maxima of the longest wavelength absorption band (see Table 2). Curve 1 (.....): compound **2e**; curve 2 (—): compound **2c**; curve 3 (---): compound **2d**; curve 4 (-.-): compound **2b**; curve 5 (---): compound **2f**; curve 6 (---): compound **2a**.

### 3.3. Fluorescence lifetimes

The data for the fluorescence lifetimes  $\tau_f$  of the investigated compounds in DCM and ETOH after excitation with 356 nm are presented in Table 3.

In DCM, the decay of the fluorescence intensity in the region of the band 'L' is monoexponential for all the compounds investigated. Similar to the steady-state fluorescence characteristics of band 'L', the fluorescence lifetime  $\tau_f$  of the 'L'-band is influenced by the structure of the corresponding pyrylium fragment. The fluorescence lifetime  $\tau_f$  of 4-CH<sub>3</sub>-compounds **1** and **1a** is about 1.9 ns, higher than  $\tau_f$  values for all the 4-Ph-substituted pyrylium salts (Scheme 1). The compounds with a fixed structure — **3**, **3a** and **4**, **4a** have a little bit longer lifetimes of their 'L'-band and  $\tau_f$  about 1.8 and 1.7 ns, respectively, in comparison to com-

pounds **2–2f**, where the  $\tau_f$  values are less than 1.6 ns. Like the  $Q_f$  values for the band 'L' (Table 2), the fluorescence lifetimes  $\tau_f$  in the region of the 'L'-band in DCM are also weakly affected by the presence of different R-substituents in the 6-styryl fragment-compounds **2a–2f**, where  $\tau_f$  vary from 1.47 ns (**2e**) to 1.58 ns (**2c**).

The fluorescence decay of the investigated PS in DCM in the region of their band 'D' is described by 3-exponential function (Table 3). The very low fluorescence quantum yield of this band for compounds **2c**, **2e**, **3a** and **4a** (Table 2) makes impossible the correct determination of their  $\tau_f$  values that is why the third column of Table 3 presents the data only for some of the investigated structures. The decay function of all the 4-Ph-substituted PS in the region of their 'D' band is dominated by a component with lifetime about 3.5 ns and amplitude more than 90%, the second component with

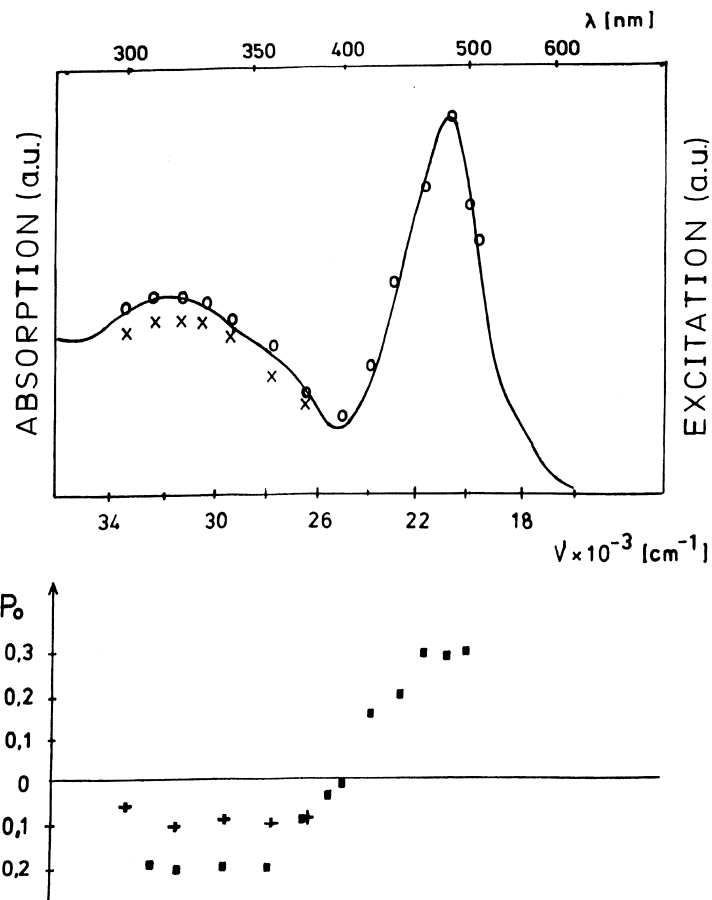


Fig. 7. Absorption spectrum of compound **1a** in ETOH at 300 K (solid line), excitation spectrum of the emission band 'D' at  $\lambda_{em}=540$  nm (○) and excitation spectrum of the emission band 'L' at  $\lambda_{em}=440$  nm (×). Lower part: Degree of polarisation  $P_0$  of compound **1a** in ETOH at 77 K, calculated from the polarisation excitation spectra of the emission band 'D' at  $\lambda_{em}=540$  nm (■), and of the emission band 'L' at  $\lambda_{em}=440$  nm (+).

Table 3

Fluorescence lifetimes  $\tau_f$  (in ns) of the investigated compounds in DCM and ETOH<sup>a</sup>

Compound	Band 'L' (in ns)	DCM <sup>b</sup>		ETOH <sup>b</sup>
		Band 'D'		Band 'L'
<b>1</b>	1.85	/c		***d
<b>1a</b>	1.89	0.99 ns/66%+3.22 ns/29%+25.9 ns/5%		***
<b>2</b>	1.56	/		0.37 ns/59%+2.66 ns/40%
<b>2a</b>	1.55	0.11 ns/5%+3.65 ns/90%+20.17 ns/5%		***
<b>2b</b>	1.52	0.22 ns/2%+3.72 ns/89%+13.8 ns/9%		0.14 ns /67%+272 ns/32%
<b>2c</b>	1.58	***		***
<b>2d</b>	1.48	0.16 ns/5%+3.74 ns/87%+14.45 ns/8%		0.19 ns /84%+3.14 ns/12%
<b>2e</b>	1.47	***		***
<b>2f</b>	1.52	0.10 ns/1%+3.12 ns/91%+17.6 ns/8%		0.47 ns /83%+2.96 ns/16%
<b>3</b>	1.76	/		***
<b>3a</b>	1.79	***		***
<b>4</b>	1.68	/		***
<b>4a</b>	1.71	***		***

<sup>a</sup> 'L' and 'D' indicate that the emission decay is measured in the maximum of the corresponding fluorescence band (see the data in Table 2). Experimental conditions: excitation wavelength=356 nm, time-resolution 0.1 ns per channel.

<sup>b</sup> In the cases of multiexponential decay, the results for the calculated  $\tau_f$  and the corresponding relative weights of decay A are presented in percent.

<sup>c</sup> Indicates the absence of 'D'-band in this compound.

<sup>d</sup> Indicates for a very low fluorescence quantum yield that makes the correct determination of  $\tau_f$  impossible.

amplitude less than 10% is long lived,  $\tau_f$  more than 13 ns, and the third component is with lifetime less than 1 ns and amplitude smaller than 5% (Table 3).

Bearing in mind that the fluorescence band 'D' is connected to the whole conjugated system of the investigated 6-styryl-substituted pyrylium salts, the multiexponential fluorescence decay in the region of this band should be attributed to different conformers, arising after the rotation in the 6-styryl fragment of the molecule.

In ETOH, the fluorescence quantum yield for most of the investigated PS is very low (Table 2) and this makes impossible to determinate their lifetimes correctly. Summarizing the available data in Table 3, it is seen that in contrary to the monoexponential decay of the 'L' band in DCM, the fluorescence decay of the band 'L' in ETOH solutions is biexponential. The decay function of the band 'L' in ETOH for compounds **2**, **2b**, **2d** and **2f** is dominated by a component with lifetime less than 1 ns and amplitude more than 60%, the lifetime of the second component is about 3 ns. As was mentioned above, the diminishing fluorescence quantum yield  $Q_f$  of band 'L' of the investigated PS in ETOH indicates for a specific solute–solvent interaction in the fluorescence excited state in protic solvents and according to the literature data [37], this could result to a complex fluorescence decay function. The observed biexponential fluorescence decay of the band 'L' in ETOH is in line with this assumption, because in DCM, where no specific interactions are observed, the fluorescence decay of the band 'L' is monoexponential (Table 3). Similar to the results in DCM, the fluorescence decay of the band 'L' in the other non-protic solvent — acetonitrile — is monoexponential, e.g. the fluorescence lifetimes  $\tau_f$  for compounds **2** and **2a** in AN ( $\lambda_{ex}=356$  nm,  $\lambda_{em}=430$  nm) are 3.15 and 3.11 ns, respectively.

#### 4. Conclusions

The experimental data for fluorescence band 'L' that is observed in the solutions of all investigated 6-styryl-substituted pyrylium salts indicate that this band should be interpreted as a local emission from the pyrylium fragment of the molecule. The following arguments support this hypothesis:

1. The energy and the shape of the fluorescence band 'L' are very close to these of the corresponding model compound of the pyrylium fragment of the molecule; the position and the shape of the fluorescence band 'L' does not depend on the substituent R in the *p*-position of the 6-styryl fragment in the pyrylium ring;
2. The fluorescence band 'L' shows mirror symmetry to the second absorption transition, which is strongly localized on the pyrylium fragment;
3. The excitation spectrum of the band 'L' coincides to the absorption spectrum of the pyrylium fragment;
4. The fluorescence lifetime of the band 'L' are only weakly influenced on the 6-styryl substituents R, the data for different R are in line with the lifetime of the corresponding

model compound that reproduces the pyrylium fragment of the molecule;

5. The effects of the proton ability of the solvent on the fluorescence quantum yield of the band 'L' and the model compound are identical — strongly decreasing  $Q_f$  in protic solvent like ETOH — the same effects are registered in MeOH;
6. The hypotheses for the local character of the emission 'L' is in agreement with the lower values of the fluorescence quantum yields  $Q_f$  of the band 'L' in comparison to  $Q_f$  of the corresponding model compound (Table 2). For the model compound the excitation with 360 nm brings the molecule directly in its fluorescent excited state  $S_1$ , while in the case of the 6-styryl-substituted compounds the fluorescence band 'L' arises after excitation in their higher excited state, most probably  $S_2$ . As a result the fluorescence quantum yield of the band 'L' is perturbed by the competition with the non-radiative internal conversion  $S_2-S_1$ .

#### Acknowledgements

The authors are grateful to Mrs. A. Poneva for the IR spectral measurements.

#### References

- [1] A.R. Katritzky (Ed.), Pyrylium Salts: Syntheses, Reactions and Physical Properties, Advances in Heterocyclic Chemistry, Supplementary 2, Academic Press, New York, 1982.
- [2] G. Dorofeenko, E. Sadekova, E. Kuznezov, Preparativnaja Khimija Pyrylievich Soleyi, Izd.Rostov. Univ., Rostov-na Donu, 1972 (in Russian).
- [3] D. Basting, F. Schaefer, B. Steyer, Appl. Phys. 3 (1974) 81.
- [4] C. Rulliere, A. Declémy, A.T. Balaban, Can. J. Phys. 63 (1985) 191.
- [5] Pol. Pat. 151 04; Chemical Abstracts 115, 258291s (1990).
- [6] Zh. Li, Zh. Zhang, Y. Teng, D. Huang, Huadong Xueyuan Xuebao, 17, 301; Chemical Abstracts 116, 153818m (1991).
- [7] Japan Kokai '84 41 363; Chemical Abstracts 100, 211659t (1984).
- [8] S. Watanabe, H. Nakazumi, S. Kado, K. Maeda, T. Kitao, J. Chem. Res. Synop. 2 (1990) 50.
- [9] P. Czerney, U.-W. Grummt, J. Chem. Res., Synop. (1996) 173.
- [10] D. Simov, S. Metzov, L. Prangova, Commun. Dept. Chem. Bulg. Acad. Sci. 19 (1986) 428.
- [11] A.T. Balaban, V. Sahimi, E. Keplinger, Tetrahedron 9 (1960) 163.
- [12] S. Parret, F. Morlet-Savary, J.P. Fouassier, K. Inomata, T. Matsumoto, F. Heisel, Bull. Chem. Soc. Jpn. 68 (1995) 2791.
- [13] G. Haucke, P. Czerney, F. Cebulla, Ber. Bunsenges. Phys. Chem. 96 (1992) 880.
- [14] D. Markovitsi, H. Sigal, C. Ecoffet, P. Millie, F. Charra, C. Fiorini, J.M. Nunzi, H. Strzelecka, M. Veber, C. Jallabert, Chem. Phys. 182 (1994) 69.
- [15] I. Lampre, S. Marguet, D. Markovitsi, S. Delysse, J.M. Nunzi, Chem. Phys. Lett. 272 (1997) 496.
- [16] S. Tripathi, M. Simalty, J. Kossanyi, Tetrahedron Lett. 26 (1985) 1995.
- [17] S. Tripathi, M. Simalty, J. Pouliquen, J. Kossanyi, Bull. Soc. Chim. Fr. (1986) 600.
- [18] I. Lampre, D. Markovitsi, C. Fiorini, F. Charra, M. Veber, J. Phys. Chem. 100 (1996) 10701.

- [19] I. Lampre, D. Markovitsi, N. Birlirakis, M. Veber, *Chem. Phys.* 202 (1996) 107.
- [20] I. Lampre, D. Markovitsi, P. Millie, *J. Phys. Chem.* 101 (1997) 90.
- [21] P. Czerney, U.W. Grummt, W. Guenther, *J. Prakt. Chem./Chem.-Ztg.* 340 (1998) 214.
- [22] F. Vollmer, W. Rettig, E. Birckner, G. Haucke, P. Czerney, *J. Inf. Rec. Mater.* 21 (1994) 497.
- [23] V. Wintgens, J. Pouliquen, J. Kossanyi, J. Williams, C. Doty, *Polym. Photochem.* 6 (1985) 1.
- [24] J. Kossanyi, P. Valat, F. Lahmadi, in: *Proceedings of the Symposium on Physical and Organic Photochemistry*, L-16, Poznan, Poland, 1995, pp. 23.07–27.07.
- [25] F. Lahmadi, P. Valat, M. Simalty, J. Kossanyi, *Res. Chem. Intermed.* 21 (1995) 807.
- [26] F. Lahmadi, P. Valat, J. Kossanyi, *New J. Chem.* 19 (1995) 965.
- [27] Y. Chen, W. Shikang, *Wuli Huaxue Xuebao*, 12, 456; *Chemical Abstracts* 125, 57785p (1996).
- [28] P.L. Nordio, A. Polimeno, G. Saielli, *J. Photochem. Photobiol. A: Chem.* 105 (1997) 69.
- [29] Z. Grabowski, K. Rotkiewicz, A. Siemiarz, D. Cowley, W. Baumann, *Nouv. J. Chim.* 3 (1979) 443.
- [30] V. Wintgens, S. Tripathi, J. Pouliquen, J. Kossanyi, *J. Photochem.* 32 (1986) 81.
- [31] S. Metzov, T. Dudev, V. Koleva, *J. Mol. Struct.* 350 (1995) 241.
- [32] I. Degani, *Boll. Sci. Fac. Chim. Ind. Bologna* 23 (1965) 21.
- [33] A.T. Balaban, G. Mateescu, M. Ellian, *Tetrahedron* 18 (1962) 1083.
- [34] T. Deligeorgiev, N. Gadjev, *Dyes and Pigments* 12 (1990) 157.
- [35] N. Borisovitch, V. Zelinskii, B. Neporent, *Dokl. Acad. Nauk USSR* 94 (1954) 37.
- [36] P. Nikolov, F. Fratev, S. Minchev, *Z. Naturforsch.* 38a (1982) 200.
- [37] P. Nikolov, I. Petkova, G. Kohler, St. Stojanov, *J. Mol. Struct.* 448 (1998) 247.
- [38] F. Perrin, *J. Phys. Radium* 7 (1926) 390.